

Kinetics and Products Distribution Study on the Catalytic Effect of Zn/HZSM-5 over Pyrolysis of *Chlorella* through TG-FTIR and Py-GC/MS

WANG Lu¹, YE Tao¹, MA Xianming¹, LIN Yan¹, CHEN Juan¹, WANG Fangbin¹, MA Peiyong^{2*}, LIU Jian^{1,3*}

1. School of Food and Biological Engineering, Hefei University of Technology, Hefei 230009, China

2. School of Mechanical Engineering, Hefei University of Technology, Hefei 230009, China

3. Engineering Research Center of Bio-process, Ministry of Education, Hefei University of Technology, Hefei 230009, China

© Science Press, Institute of Engineering Thermophysics, CAS and Springer-Verlag GmbH Germany, part of Springer Nature 2023

Abstract: In this study, both the pyrolysis and catalytic pyrolysis behaviour of *chlorella* were investigated using thermogravimetric analysis combined with Fourier Transform Infrared spectrum (TG-FTIR) and Py-GC/MS. The results of TG indicated the pyrolysis of *chlorella* was divided into three stages, and the Coats-Redfern kinetic model was used for the analysis and validation of the obtained thermal data. The regression coefficients indicated that the pyrolysis of *chlorella* was close to second-order reaction. The activation energy of pyrolysis of *chlorella* and catalytic pyrolysis of *chlorella*+HZSM-5, *chlorella*+Zn/HZSM-5 was 61.645, 59.080 and 56.808 kJ·mol⁻¹, respectively. Combined with the data of FTIR, we found that the addition of the HZSM-5 effectively reduced the activation energy required by pyrolysis; the addition of the Zn/HZSM-5 could not only reduce the activation energy, but also reduce the yield of oxygen-containing compounds, increase the emissions of CO₂, and facilitate the production of high value-added hydrocarbon products. These results were also verified by Py-GC/MS that the addition of Zn/HZSM-5 could reduce the formation of ketones and aldehydes and increase the production of nitrogen-containing compounds. Thus, through the catalytic pyrolysis of *chlorella*, the utilization range of *chlorella* can be expanded, and better bio-oil can be obtained, which will play a crucial role in the selection of available energy in the future.

Keywords: catalytic pyrolysis, *chlorella*, TG-FTIR, kinetic, Zn/HZSM-5, Py-GC/MS

1. Introduction

In recent decades, the increasing population and the rapidly developing industrialization had led to a large consumption of energy resources. Biomass, as a clean, renewable, and sustainable resource, has been regarded as the best alternative to fossil fuels [1]. Bio-fuel derived

from algae, in particular, has been already used in many applications because they can be produced in large quantities without affecting the environment [2]. It is reported that compared with other biomass, *chlorella* species can be planted in large areas [3], grow fast, and most importantly, it has a high conversion rate of bio-fuel [4].

Received: Aug 16, 2021
AE: LI Yinshi

Corresponding author: MA Peiyong;
LIU Jian

E-mail: mapeiyong@163.com
liujian509@hfut.edu.cn
www.springerlink.com

Algae can be converted into bio-fuel via thermochemical processes [5, 6] such as pyrolysis, combustion, gasification, torrefaction and liquefaction. Of all thermochemical processes, pyrolysis [7, 8] is a promising and meaning method in biomass conversion. This process includes different kinds of reactions, which is influenced by temperature, heating rate, residence time, and feedstock composition [9–12]. The pyrolytic bio-oil of microalgae contains many kinds of organic compounds, such as nitrogenated compounds (amides, amines, and heterocyclic compounds containing nitrogen), oxygenated compounds (carboxylic acids, carboxides, and phenols), and hydrocarbons (like benzene, alkane, and alkene). Microalgae, that carbon content is about 51%–81.6%, with a median value of 62.3%, the hydrogen content is 6.7%–12%, and the nitrogen content is 5.2%–16.3% [13]. Compared with the bio-oils produced from other biomass, the microalgal bio-oil contains much less oxygen content, a higher high heating value (HHV), and even more nitrogen content, because protein and lipid contents of algae are higher than the other traditional biomass resources [4, 14].

Thermogravimetric analysis (TGA) [15], differential thermal analysis (DTA) and differential scanning calorimetry (DSC) is widely used in the thermal behaviour of biomass. The thermogravimetric (TG) data measures the variation of amount and rate of decomposition with time and temperature. And TGA data is very important for the determination of kinetic parameters of pyrolysis reactions that is extremely useful for the design and operation of thermochemical conversion systems [16–18].

Understanding the volatile compounds released during the pyrolysis of biomass is of great significance for determining the reaction temperature and residence time in the later comprehensive utilization of biomass [19]. Toward this end, Fourier Transform Infrared Spectrum (FTIR), Mass Spectrum (MS) [20] have been combined with TG, and these can analyse not only the mass loss but also the composition of volatile compounds released during pyrolysis in real-time. From the obtained FTIR spectrum, the corresponding functional groups and contents can be determined for qualitative and quantitative analysis of the pyrolysis products at different stages [21, 22]. Py-GC/MS are also used to determine whether the volatile substances in the pyrolysis products contain valuable substances. According to the obtained mass spectrum, the type and content of compounds can be determined, which is very helpful for the recovery and utilization of pyrolysis products [23].

HZSM-5 is a recognized catalyst for catalytic conversion of biomass, with good acid resistance and heat resistance [24]. However, when HZSM-5 is used as catalyst alone, there are still many problems in product

quality caused by its acidity. It is found that the metal modified catalyst can effectively solve these problems by simple impregnation method. The modification of the metal can significantly change the acidic properties of HZSM-5, thus promoting the catalytic reaction [25]. Metals commonly used in modification include nickel, palladium [26], iron, zinc [27, 28], etc. It has been found that HZSM-5 modified with nickel, cobalt, zinc, and other metals can effectively reduce the yield of oxygen-containing compounds, which has a positive impact on the high value-added oil phase generated by pyrolysis [25].

In our previous study, we had found the modification of zinc on HZSM-5 had a positive effect on nitrogen-containing compounds (NCCs) and hydrocarbons of *chlorella* by pyrolysis [29]. But the mechanism has rarely been studied. Therefore, in this study, kinetic and products distribution of the catalytic pyrolysis of *chlorella* with Zn/HZSM-5 as the catalyst was studied by TG-FTIR and Py-GC/MS, and the aim of this study was to determine the role of Zn/HZSM-5 in the catalytic pyrolysis of *chlorella*.

2. Experiment Materials and Methods

2.1. Biomass and catalyst preparation.

The microalgae feedstock, *chlorella*, purchased from Wudi Ivqi Bio Engineering Inc., China, with green food grade. The composition, proximate, and elemental analysis of the *chlorella* were shown in our previous work [29]. The biomass was dried at 100°C for 24 h to remove the moisture content and then sieved to a particle size no more than 200 μm . The zeolite catalyst, HZSM-5, which was purchased from Nankai University. The catalyst was calcinated in the muffle furnace for 4 h at 550°C and sieved to a particle size less than 425 μm before use. The surface area of the HZSM-5 catalyst was measured to be 350 $\text{m}^2\cdot\text{g}^{-1}$. And catalyst Zn/HZSM-5 was prepared by Zn (NO_3)₂ and HZSM-5 by impregnating.

2.2 Thermal behaviour

The kinetics data derived from TGA are very important for the efficient design and analysis of the pyrolysis process [30]. The pyrolysis experiments were performed with a constant heating rate of 20°C·min⁻¹ using the thermogravimetric analyzer (STA449F5, Netzsch Group). For this test, we prepared the samples include *chlorella*, *chlorella*+HZSM-5 mixed in 1:1 and *chlorella*+Zn/HZSM-5 mixed in 1:1. 10 mg samples were loaded into an alumina crucible and heated from 25°C to 600°C with a nitrogen flow rate of 20 mL·min⁻¹. The TG-FTIR instrument (Nexus 670 spectrometer, Nicolet Group), which was used to analyze gaseous products released during pyrolysis.

2.3 Kinetics of pyrolysis

In this study, the pyrolysis data was obtained at a constant heating rate ($20^{\circ}\text{C}\cdot\text{min}^{-1}$). Char and volatiles were produced during the pyrolysis of biomass and the reaction process is as follows:



The mass loss rate of *chlorella* could be calculated by:

$$\frac{dW}{dt} = -\frac{1}{W_0} \left(\frac{dW_t}{dt} \right) \quad (2)$$

α means the change in the mass of *chlorella*, could be calculated by Eq. (3):

$$\alpha = \frac{W_0 - W_t}{W_0 - W_f} \quad (3)$$

where W_0 is the initial mass of the biomass sample; W_t is the mass of the sample at the relevant time; W_f is the final mass of the sample at the end of reaction [31]. There is a linear relationship between the degradation rate and the reaction rate constant k from Eq. (4), and kinetic parameter is described by the Arrhenius expression as follows [32–34]:

$$\frac{d\alpha}{dt} = kf(\alpha) \quad (4)$$

$$k = Ae^{-E_A/RT} \quad (5)$$

where A is the pre-exponential factor (s^{-1}); E_A is the activation energy ($\text{J}\cdot\text{mol}^{-1}$); R is the universal gas constant ($8.314 \text{ J}\cdot\text{mol}^{-1}\cdot\text{K}^{-1}$), and T is the absolute temperature (K). Substitute Eq. (4) into Eq. (5), the new formula is as follows:

$$\frac{d\alpha}{dt} = Ae^{\frac{-E_A}{RT}} \cdot f(\alpha) \quad (6)$$

Under constant heating rate, β is defined as

$$\beta = \frac{dT}{dt} \quad (7)$$

Combining Eqs. (6) and (7) gives:

$$\frac{d\alpha}{dT} = \frac{A}{\beta} e^{\frac{-E_A}{RT}} \cdot f(\alpha) \quad (8)$$

Then, the values of E_A and A were obtained by multiple rates iso-temperature method (iso-conversion rate method) and calculated by the Coats-Redfern model. The equation as follows:

$$\ln \left[\frac{1}{T^2} \frac{1-(1-\alpha)^{1-n}}{1-n} \right] = \ln \frac{AR}{\beta E_A} - \frac{E_A}{RT} \quad n \neq 1 \quad (9)$$

$$\ln \left[\frac{-\ln(1-\alpha)}{T^2} \right] = \ln \frac{AR}{\beta E_A} - \frac{E_A}{RT} \quad n = 1 \quad (10)$$

2.4 Py-GC/MS

Py-GC/MS analysis was delegated to the SLIntelligent Analysis Testing Center (Nanjing, China). 1 mg feedstock was to prepared complete the test. For the part of pyrolysis, the furnace temperature was set to 270°C and the heating wire temperature was set to 500°C . For the part of GC/MS, a helium atmosphere with a flow rate of $1 \text{ mL}\cdot\text{min}^{-1}$ was required in the instrument and ensured a split ratio of 50:1. The nozzle temperature of instrument was set at 250°C ; the oven temperature was set to 40°C at first, then maintained 1 min and started to heat up to 280°C at $6^{\circ}\text{C}\cdot\text{min}^{-1}$. Finally, the final temperature was kept for 15 min.

3. Results and Discussion

3.1 Pyrolysis and catalytic pyrolysis behavior of *chlorella*

To better figure out the thermal decomposition behavior and its mechanism, we apply the TG analysis to show the relationship between the weight of the sample and the temperature. One heating rate is set to study the pyrolysis of *chlorella*, and the TG curves and DTG curves are shown in Fig. 1. To better understand the pyrolysis behavior of the *chlorella* with the addition of different catalysts, the influences of quality of catalysts on the result are excluded, the result of weight deducted (DW) TG and DTG curves are represented in Fig. 1 by dashed lines. And the pyrolysis character parameters of

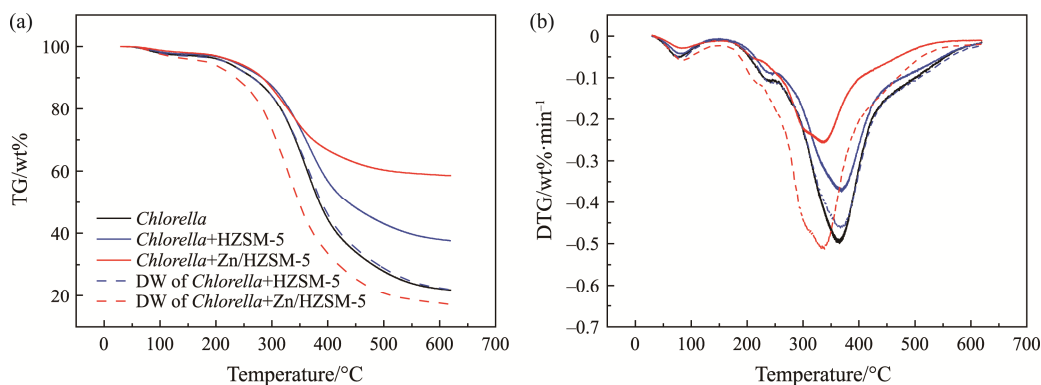


Fig. 1 (a) TG curves of *chlorella*, *chlorella*+HZSM-5 and *chlorella*+Zn/HZSM-5. (b) DTG curves of *chlorella*, *chlorella*+HZSM-5 and *chlorella*+Zn/HZSM-5

Table 1 Pyrolysis characters of *chlorella*, DW of *chlorella*+HZSM-5 and DW of *chlorella*+Zn/HZSM-5

Feedstock	¹ D _{max}	² T _{max}	³ ML ₁	⁴ ML ₂	⁵ ML ₃	⁶ ML _{Total}
<i>chlorella</i>	0.498	364.29	2.893	69.291	5.963	78.147
DW of <i>chlorella</i> +HZSM-5	0.467	369.04	3.062	68.087	6.788	77.937
DW of <i>chlorella</i> +Zn/HZSM-5	0.513	334.29	4.003	75.245	3.594	82.842

¹The maximum pyrolysis rate (wt.%/min). ²The temperature of the maximum pyrolysis rate (°C). ³Mass loss of the first stage (25°C–150°C) (wt.%).

⁴Mass loss of the second stage (150°C–500°C) (wt.%). ⁵Mass loss of the third stage (500°C–600°C) (wt.%). ⁶Total mass loss (wt.%).

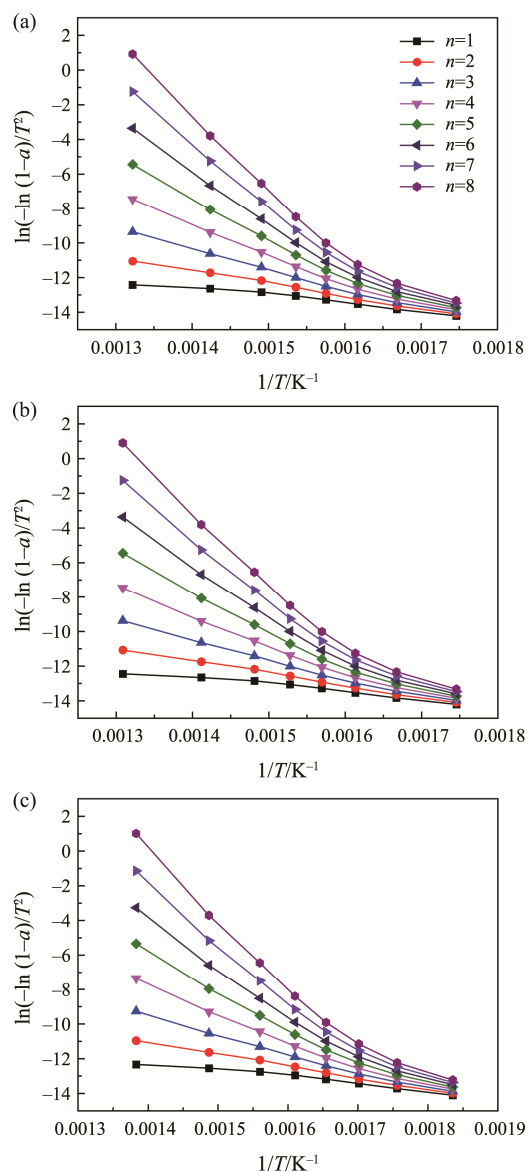
chlorella, DW of *chlorella*+HZSM-5 and DW of *chlorella*+Zn/HZSM-5 pyrolysis process are listed in Table 1, respectively. As seen in Fig. 1(a), mass loss below 150°C is due to the evaporation of moisture. The maximum mass loss of *chlorella* occurs between 150°C and 500°C; this phenomenon is caused by the first decomposition of organic matter [35]. The substances decomposed at this stage are mainly three organic substances: carbohydrates, protein, and lipids [36]. The last stage of pyrolysis ranges from 500°C to 600°C (or even up to 800°C) [37, 38]. The mass loss occurs at a very slow rate; this phenomenon may relate to the decomposition of the carbonaceous materials and retention of the char [39]. It is clear to see that the TG curve of *chlorella*+HZSM-5 is not significantly different from the TG curve of *chlorella*, while the result of *chlorella*+Zn/HZSM-5 present an earlier reaction, and there is less deposition of carbon, and the pyrolysis process are more complete.

It is observed from Fig. 1(b) that the addition of HZSM-5 has rare effect on the temperature corresponding to the maximum pyrolysis rate, while the addition of Zn/HZSM-5 reduces the temperature corresponding to the maximum pyrolysis rate and increases the maximum pyrolysis rate. It is reported that an increase in the maximum pyrolysis rate means an increase in the sample reactivity [40]. In summary, the addition of the Zn/HZSM-5 effectively reduces the content of carbon deposition in the pyrolysis products of *chlorella*, at the same time advance and complete pyrolysis are at lower temperature.

3.2 Coats-Redfern analysis

To further understand the catalytic pyrolysis between *chlorella* and catalyst, we use the Coats-Redfern model to characterize the catalytic effect as shown in Fig. 2. According to Coats-Redfern method, the corresponding values of different reaction orders are calculated based on these data and the equations mentioned above, and the calculated activation energy (E_A) is listed in Table 2.

It is clear to see that with the reaction order increases, the activation energy also increases. The highest regression coefficients (R^2) for three types of *chlorella* pyrolysis are 0.9962, 0.997 and 0.9981, respectively. We can confirm that the pyrolysis of *chlorella* is close to

**Fig. 2** Coats-Redfern model of (a) *chlorella*, (b) *chlorella*+HZSM-5 and (c) *chlorella*+Zn/HZSM-5

second-order reaction due to their highest R^2 value. Activation energy is the minimum energy require for the molecule to get close to the reaction to form the product [41]. The activation energy for the *chlorella* pyrolysis is 61.564 kJ·mol⁻¹, while the activation energy for the *chlorella*+HZSM-5 catalytic pyrolysis and *chlorella*+

Table 2 The value of E_A , R^2 of *chlorella*, *chlorella*+HZSM-5 and *chlorella*+Zn/HZSM-5 calculated by the Coats-Redfern method

Feedstock	n	Coats-Redfern method	
		$E_A/\text{kJ}\cdot\text{mol}^{-1}$	R^2
<i>Chlorella</i>	1	36.490 15	0.9627
	2	61.564 34	0.9962
	3	93.249 82	0.9898
<i>Chlorella</i> +HZSM-5	1	34.854 78	0.964
	2	59.060 16	0.997
	3	89.641 55	0.9898
<i>Chlorella</i> +Zn/HZSM-5	1	33.576 09	0.9657
	2	56.808 73	0.9981
	3	86.157 98	0.9907

Zn/HZSM-5 catalytic pyrolysis is 59.080 and 56.808 $\text{kJ}\cdot\text{mol}^{-1}$, respectively. It could be obtained that the activation energy of the catalytic pyrolysis is lower than the non-catalytic pyrolysis. It means that the Zn/HZSM-5 have the apparent effect on reducing the energy for pyrolysis of *chlorella*.

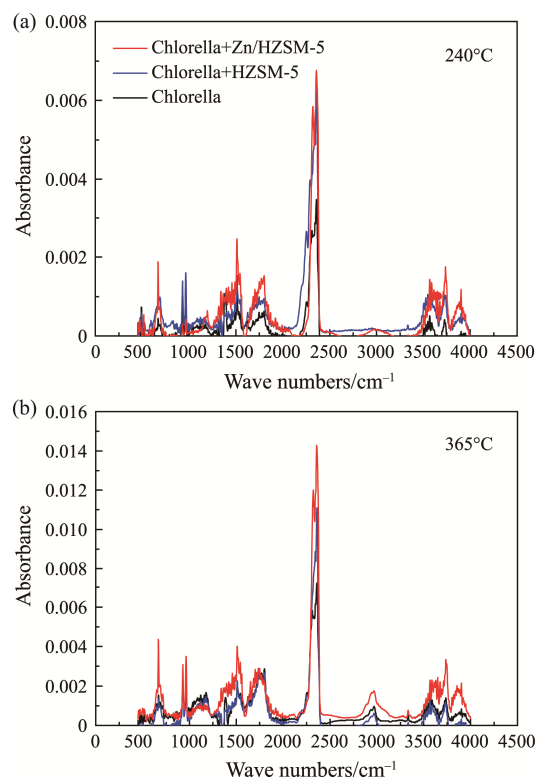
3.3 TG-FTIR analysis

The evolvement of the volatile compounds during the thermal decomposition of *chlorella*, *chlorella*+HZSM-5 and *chlorella*+Zn/HZSM-5 is detected by the method of real time FT-IR. 240°C and 365°C are chosen based on the mass loss process from the inflection points of DTG curves in Fig. 1(b), and the FT-IR result at these two temperatures is shown in Fig. 3.

From Fig. 3, it's obvious that adsorption peak between 4000 cm^{-1} and 3400 cm^{-1} are the characteristics signals of water. There's no formation of water until 150°C. The absorbances slightly increase with the increasing temperature. As the temperature increases, the ring-opening, depolymerization, recondensation, and depolymerization reactions occur. Adsorption peak at 2800–3000 cm^{-1} is ascribed to saturated hydrocarbon bonds ($-\text{CH}_4$, $-\text{CH}_3$ and $-\text{CH}_2$). The formation of hydrocarbons is observed at 365°C, but not 240°C, because C-O and C=O bonds are much more likely to break at low temperatures than C-C and C-H bonds [42]. CO_2 has characteristic adsorption peak at 660 cm^{-1} and 2358 cm^{-1} , and more CO_2 is released during pyrolysis of *chlorella*+HZSM-5 and *chlorella*+Zn/HZSM-5 compared with the pyrolysis of *chlorella*. This is probably because the addition of catalysts may facilitate devolatilization and decarboxylation. The absorbance peak between 1750 cm^{-1} and 1650 cm^{-1} correspond to the C=O carbonyl stretching of carboxylic acid or carboxide groups. As *chlorella* contains a large amount of carboxylic acid, it is speculated that these signals are the representative of carboxylic groups. Moreover, the peak at 1740 cm^{-1} at higher temperatures correspond to esters formed from the

reaction between carboxylic acids and alcohols, both of which are observed in the fingerprint region between 1200 cm^{-1} and 1000 cm^{-1} .

From the FTIR spectrum of two temperatures, compared with pyrolysis of only *chlorella*, addition of HZSM-5 and Zn/HZSM-5 facilitate the production of high value-added hydrocarbon products. Zn/HZSM-5 show more obvious enhancement than HZSM-5.

**Fig. 3** The FTIR spectrum of gaseous product from *chlorella*, *chlorella*+HZSM-5 and *chlorella*+Zn/HZSM-5 at 240°C and 365°C

3.4 Py-GC/MS analysis

Py-GC/MS is used to analyze the composition of *chlorella* pyrolysis products before and after adding catalysts, and the results are shown in the Fig. 4. The main pyrolysis products are classified and list in Table 3, and their peak areas are compared as shown in Fig. 5.

It is noteworthy that after adding the HZSM-5 and Zn/HZSM-5, the content of acid, esters, aldehydes, and ketones go down, while the contents of alkyl benzenes and NCCs increase significantly. The acids decrease from 28.68% to 28.25% and 25.19% in the area, the content of aldehydes and ketones decrease from 10.58% to 9.84% and 6.82% in the area, and the content of esters reduces greatly from 19.97% to 1.93% and 1.62% in the area, respectively. The content of alkyl benzenes increases from 1.67% to 5.93% and 7.68% in the area, and the content of NCCs increases from 3.23% to 19.06% and 21.27% in the area, respectively.

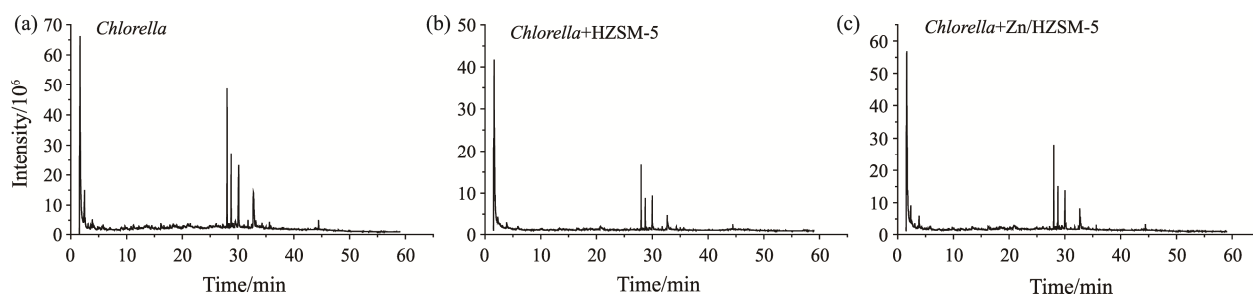


Fig. 4 Py-GC/MS analysis of pyrolysis products of (a) *chlorella*, (b) *chlorella*+HZSM-5 and (c) *chlorella*+Zn/HZSM-5

Table 3 The peak area (%) of the pyrolysis products of *chlorella*, *chlorella*+HZSM-5 and *chlorella*+Zn/HZSM-5

Compounds	Retain time /min	Peak area/%		
		<i>Chlorella</i>	<i>Chlorella</i> +HZSM-5	<i>Chlorella</i> +Zn/HZSM-5
Acids				
Acetic acid	2.455	9.79	6.44	4.49
Butanoic acid, 3-methyl-	5.813	0.78		
4-Pentenoic acid	7.027	0.53		
trans-2-Hexadecenoic acid	27.255	1.05		
n-Hexadecanoic acid	30.099	15.62	12.54	12.26
9,12-Octadecadienoic acid (Z,Z)-	32.668		5.07	5.46
9,12,15-Octadecatrienoic acid, (Z,Z,Z)-	32.748	0.91		2.98
cis-Vaccenic acid	32.776		4.2	
NCCs				
Acetonitrile	1.818		19.06	16.9
Pyrrole	3.606	0.62		
Pentanenitrile, 4-methyl-	4.822	0.37		
Indole	16.148	1.13		3.27
Tetradecanenitrile	28.656			1.1
Octadecanamide	33.206	1.11		
Esters and Cyclic esters				
Propanoic acid, 2-oxo-, methyl ester	3.94	0.55		
9,12-Hexadecadienoic acid, methyl ester	29.428			0.41
Oxacycloheptadec-8-en-2-one	29.44	0.8		
Cyclopropanecarboxylic acid, tridec-2-ynyl ester	30.179			0.75
Octadecanoic acid, 2-propenyl ester	31.772	0.89	0.75	0.46
9,12-Octadecadienoic acid, methyl ester	32.749	17.1		
Isopropyl linoleate	34.297	0.63	0.54	
Hexadecanoic acid, 1-(hydroxymethyl)-1,2-ethanediyl ester	35.004		0.64	
Aldehydes and Ketones				
Propanal, 2-methyl-	1.960	4.73	5.66	3.68
2,3-Butanedione	2.115	2.99	3.57	1.28
Butanal, 3-methyl-	2.460		0.61	0.78
2-Pentanone, 4,4-dimethyl-	2.542	2.51		
Ethanone, 1-(methylenecyclopropyl)-	3.077			1.08
Ethanone, 1-[2-methyl-5-(1-methylethenyl)cyclopentyl]-, (1. alpha., 2. alpha., 5. beta.)-	28.113	0.35		
Alkyl benzenes				
Toluene	3.837	1.67	3.05	4.36
o-Xylene	5.859		2.88	3.5

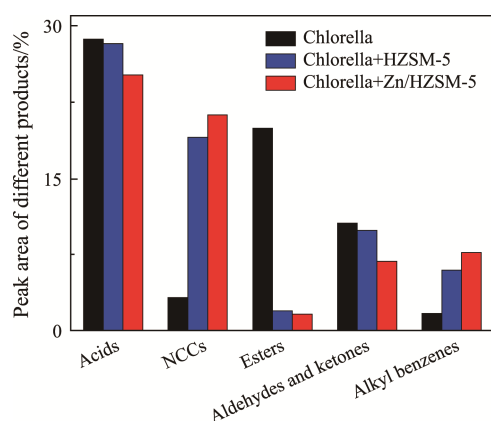


Fig. 5 The peak area (%) of the different pyrolysis products of *chlorella*, *chlorella*+HZSM-5 and *chlorella*+Zn/HZSM-5

These results show that the catalysts promote degradation of oxygen-containing compounds (acid, esters, aldehydes, and ketones). The reason for the increase in NCCs is that the *chlorella* contains a large amount of protein; these proteins are converted into different kinds of amino acids during pyrolysis [43]. Some of the small amino acids are converted to volatiles gases (NH_3 , CO_2 and H_2O) [44], which combine with fatty acids in *chlorella* to form amides and turn them into nitriles [45]. Nitrogen heterocyclic substances such as indoles are mainly produced by the pyrolysis of phenylalanine and tyrosine [46].

In summary, the use of Zn/HZSM-5 as a catalyst for *chlorella* pyrolysis can decrease oxygen-containing compounds in the products, improve the generation of NCCs, and enhance the comprehensive utilization value of *chlorella*.

4. Conclusion

In this study, the pyrolysis of *chlorella*, catalytic pyrolysis of *chlorella*+HZSM-5 and catalytic pyrolysis of *chlorella*+Zn/HZSM-5 was studied contrastively. TG-FTIR and Py-GC/MS was carried out for analysis. TG analysis showed the primary devolatilization step of *chlorella* occurred between temperatures of 150°C and 500°C. The pyrolysis of *chlorella* followed the second order reaction model. E_A values of *chlorella*+Zn/HZSM-5 calculated by Coats-Redfern model was lower than *chlorella* and *chlorella*+HZSM-5. It indicated Zn/HZSM-5 could promote reaction more effectively. FTIR spectrum revealed that the content of gaseous products released during pyrolysis changed with addition of catalysts. Addition of Zn/HZSM-5 facilitated the devolatilization and decarboxylation; more hydrocarbon was generated then. Py-GC/MS result showed the addition of Zn/HZSM-5 could decrease the

formation of acids, esters, ketones, and aldehydes effectively and increase the production of NCCs. Combining the results of FT-IR and Py-GC/MS, it is easy to see that the addition of Zn/HZSM-5 makes *chlorella* produce many valuable products. It is a very potential application of the deep processing of the *chlorella*.

Acknowledgements

This study was supported by the National Natural Science Foundation of China (31901406), the Fundamental Research Funds for the Central Universities (JZ2020HGTB0044), Major R&D projects of key technologies of Hefei (J2019G22).

Conflict of Interest

On behalf of all authors, the corresponding author states that there is no conflict of interest.

References

- [1] Sirajunnisa A.R., Surendhiran D., Algae - A quintessential and positive resource of bioethanol production: A comprehensive review. *Renewable & Sustainable Energy Reviews*, 2016, 66: 248–267.
- [2] Suganya T., Varman M., Masjuki H.H., et al., Macroalgae and microalgae as a potential source for commercial applications along with biofuels production: A biorefinery approach. *Renewable & Sustainable Energy Reviews*, 2016, 55: 909–941.
- [3] Saber M., Nakhshinev B., Yoshikawa K., A review of production and upgrading of algal bio-oil. *Renewable & Sustainable Energy Reviews*, 2016, 58: 918–930.
- [4] Thangalazhy-Gopakumar S., Adhikari S., Chattanathan S. A., et al., Catalytic pyrolysis of green algae for hydrocarbon production using H(+)ZSM-5 catalyst. *Bioresource Technology*, 2012, 118: 150–157.
- [5] Jayaraman K., Kok M.V., Gokalp I., Pyrolysis, combustion and gasification studies of different sized coal particles using TGA-MS. *Applied Thermal Engineering*, 2017, 125: 1446–1455.
- [6] Durak H., Thermochemical conversion of *Phellinus pomaceus* via supercritical fluid extraction and pyrolysis processes. *Energy Conversion and Management*, 2015, 99: 282–298.
- [7] Aysu T., Durak H., Catalytic pyrolysis of liquorice (*Glycyrrhiza glabra* L.) in a fixed-bed reactor: Effects of pyrolysis parameters on product yields and character. *Journal of Analytical and Applied Pyrolysis*, 2015, 111: 156–172.
- [8] Durak H., Genel S., Tunç M., Pyrolysis of black cumin seed: Significance of catalyst and temperature product

- yields and chromatographic characterization. *Journal of Liquid Chromatography & Related Technologies*, 2019, 42(11–12): 331–350.
- [9] Bhola V., Desikan R., Santosh S.K., et al., Effects of parameters affecting biomass yield and thermal behaviour of *Chlorella vulgaris*. *Journal of Bioscience and Bioengineering*, 2011, 111(3): 377–382.
- [10] Duan P.G., Jin B.B., Xu Y.P., et al., Co-pyrolysis of microalgae and waste rubber tire in supercritical ethanol. *Chemical Engineering Journal*, 2015, 269: 262–271.
- [11] Li G., Zhou Y. G., Ji F., et al., Yield and characteristics of pyrolysis products obtained from schizochytrium limacinum under different temperature regimes. *Energies*, 2013, 6(7): 3339–3352.
- [12] Muradov N., Fidalgo B., Gujar A.C., et al., Pyrolysis of fast-growing aquatic biomass - *Lemna minor* (duckweed): Characterization of pyrolysis products. *Bioresource Technology*, 2010, 101(21): 8424–8428.
- [13] Yang C.Y., Li R., Zhang B., et al., Pyrolysis of microalgae: A critical review. *Fuel Processing Technology*, 2019, 186: 53–72.
- [14] Rajanren J.R., Ismail H.M., Narayanapillai P.T., Investigation on phototrophic growth of an indigenous *Chlorella vulgaris* for biodiesel production. *Environmental Progress & Sustainable Energy*, 2015, 34(4): 1215–1220.
- [15] Kok M.V., Özgür E., Thermal analysis and kinetics of biomass samples. *Fuel Processing Technology*, 2013, 106: 739–743.
- [16] Jaroenphasemmesuk C., Tippayawong N., Thermal degradation kinetics of sawdust under intermediate heating rates. *Applied Thermal Engineering*, 2016, 103: 170–176.
- [17] Liu G.C., Liao Y.F., Guo S.D., et al., Thermal behavior and kinetics of municipal solid waste during pyrolysis and combustion process. *Applied Thermal Engineering*, 2016, 98: 400–408.
- [18] Oladokun O., Ahmad A., Abdullah T.A.T., et al., Multicomponent devolatilization kinetics and thermal conversion of *Imperata cylindrica*. *Applied Thermal Engineering*, 2016, 105: 931–940.
- [19] Gai C., Zhang Y.H., Chen W.T., et al., Thermogravimetric and kinetic analysis of thermal decomposition characteristics of low-lipid microalgae. *Bioresource Technology*, 2013, 150: 139–148.
- [20] Jayaraman K., Kok M.V., Gokalp I., Thermogravimetric and mass spectrometric (TG-MS) analysis and kinetics of coal-biomass blends. *Renewable Energy*, 2017, 101: 293–300.
- [21] Gao Y.J., Chen X., Zhang J.G., et al., Chitin-derived mesoporous, nitrogen-containing carbon for heavy-metal removal and styrene epoxidation. *Chempluschem*, 2015, 80(10): 1556–1564.
- [22] Lin B.C., Wang J., Huang Q.X., et al., Aromatic recovery from distillate oil of oily sludge through catalytic pyrolysis over Zn modified HZSM-5 zeolites. *Journal of Analytical and Applied Pyrolysis*, 2017, 128: 291–303.
- [23] Lv X.C., Liu H.C., Huang Y.Q., et al., Synergistic effects on co-pyrolysis of low-temperature hydrothermally pretreated high-protein microalgae and polypropylene. *Energy Conversion and Management*, 2021, 229: 13.
- [24] Jae J., Tompsett G.A., Foster A.J., et al., Investigation into the shape selectivity of zeolite catalysts for biomass conversion. *Journal of Catalysis*, 2011, 279(2): 257–268.
- [25] Zheng Y.W., Wang F., Yang X.Q., et al., Study on aromatics production via the catalytic pyrolysis vapor upgrading of biomass using metal-loaded modified H-ZSM-5. *Journal of Analytical and Applied Pyrolysis*, 2017, 126: 169–179.
- [26] Iliopoulou E.F., Stefanidis S.D., Kalogiannis K.G., et al., Catalytic upgrading of biomass pyrolysis vapors using transition metal-modified ZSM-5 zeolite. *Applied Catalysis B-Environmental*, 2012, 127: 281–290.
- [27] Espindola J.S., Gilbert C.J., Perez-Lopez O.W., et al., Conversion of furan over gallium and zinc promoted ZSM-5: The effect of metal and acid sites. *Fuel Processing Technology*, 2020, 201: 11.
- [28] Fanchiang W.L., Lin Y.C., Catalytic fast pyrolysis of furfural over H-ZSM-5 and Zn/H-ZSM-5 catalysts. *Applied Catalysis a-General*, 2012, 419: 102–110.
- [29] Wu H.H., Wang L., Ji G.B., et al., Renewable production of nitrogen-containing compounds and hydrocarbons from catalytic microwave-assisted pyrolysis of *chlorella* over metal-doped HZSM-5 catalysts. *Journal of Analytical and Applied Pyrolysis*, 2020, 151: 7.
- [30] Liang Y.G., Cheng B.J., Si Y.B., et al., Thermal decomposition kinetics and characteristics of *Spartina alterniflora* via thermogravimetric analysis. *Renewable Energy*, 2014, 68: 111–117.
- [31] Agrawal A., Chakraborty S., A kinetic study of pyrolysis and combustion of microalgae *Chlorella vulgaris* using thermo-gravimetric analysis. *Bioresource Technology*, 2013, 128: 72–80.
- [32] Lopez-Gonzalez D., Fernandez-Lopez M., Valverde J. L., et al., Kinetic analysis and thermal characterization of the microalgae combustion process by thermal analysis coupled to mass spectrometry. *Applied Energy*, 2014, 114: 227–237.
- [33] Sharara M.A., Holeman N., Sadaka S.S., et al., Pyrolysis kinetics of algal consortia grown using swine manure wastewater. *Bioresource Technology*, 2014, 169: 658–666.
- [34] Zou S.P., Wu Y.L., Yang M.D., et al., Pyrolysis characteristics and kinetics of the marine microalgae *Dunaliella tertiolecta* using thermogravimetric analyzer.

- Bioresource Technology, 2010, 101(1): 359–365.
- [35] Naqvi S.R., Uemura Y., Osman N., et al., Kinetic study of the catalytic pyrolysis of paddy husk by use of thermogravimetric data and the Coats-Redfern model. *Research on Chemical Intermediates*, 2015, 41(12): 9743–9755.
- [36] Azizi K., Moraveji M.K., Najafabadi H.A., Characteristics and kinetics study of simultaneous pyrolysis of microalgae *Chlorella vulgaris*, wood and polypropylene through TGA. *Bioresource Technology*, 2017, 243: 481–491.
- [37] Chen W.H., Lin B.J., Characteristics of products from the pyrolysis of oil palm fiber and its pellets in nitrogen and carbon dioxide atmospheres. *Energy*, 2016, 94: 569–578.
- [38] Fong M.J.B., Loy A.C.M., Chin B.L.F., et al., Catalytic pyrolysis of *Chlorella vulgaris*: Kinetic and thermodynamic analysis. *Bioresource Technology*, 2019, 289: 121689.
- [39] Liu Y.Q., Lim L.R.X., Wang J., et al., Investigation on pyrolysis of microalgae *botryococcus braunii* and *hapalosiphon* sp. *Industrial & Engineering Chemistry Research*, 2012, 51(31): 10320–10326.
- [40] Jayaraman K., Kok M.V., Gokalp I., Combustion properties and kinetics of different biomass samples using TG-MS technique. *Journal of Thermal Analysis and Calorimetry*, 2016, 127(2): 1361–1370.
- [41] Wang L., Lei H.W., Liu J., et al., Thermal decomposition behavior and kinetics for pyrolysis and catalytic pyrolysis of Douglas fir. *RSC Advances*, 2018, 8(4): 2196–2202.
- [42] Qiao Y., Wang B., Zong P., et al., Thermal behavior, kinetics and fast pyrolysis characteristics of palm oil: Analytical TG-FTIR and Py-GC/MS study. *Energy Conversion and Management*, 2019, 199: 111964.
- [43] Zhang W.G., Zhang Z.H., Yan S.H., Effects of various amino acids as organic nitrogen sources on the growth and biochemical composition of *Chlorella pyrenoidosa*. *Bioresource Technology*, 2015, 197: 458–464.
- [44] Simmonds P.G., Medley E.E., Ratcliff M.A., et al., Thermal decomposition of aliphatic monoaminomonocarboxylic acids. *Analytical Chemistry*, 1972, 44(12): 2060–2066.
- [45] Anand V., Sunjeev V., Vinu R. Catalytic fast pyrolysis of *Arthrospira platensis* (spirulina) algae using zeolites. *Journal of Analytical and Applied Pyrolysis*, 2016, 118: 298–307.
- [46] Debono O., Villot A., Nitrogen products and reaction pathway of nitrogen compounds during the pyrolysis of various organic wastes. *Journal of Analytical and Applied Pyrolysis*, 2015, 114: 222–234.